Ren, Mingfa, Huang, Qizhong, Liu, Changzhi, & Li, Tong
(2015)
Numerical optimization of soft-mold aided co-curing process of advanced grid-stiffened composite structures.
Journal of Reinforced Plastics and Composites, *34*(21), pp. 1765-1778.

http://doi.org/10.1177/0731684415597075

Numerical optimization of soft-mold aided co-curing process of advanced grid-stiffened composite structures

Mingfa Ren[1], Qizhong Huang[2], Changzhi Liu[1] and Tong Li[3,*]

[1]State Key Laboratory of Structural Analysis for Industrial Equipment, Dalian University of Technology, Dalian, China

[2]State key laboratory of special reinforce fiber composite material, Beijing Composite Materials Co., Ltd, Beijing, China

[3]School of Chemistry, Physics and Mechanical Engineering, Queensland University of Technology, Brisbane, Australia

Abstract: The co-curing process for advanced grid-stiffened (AGS) composite structure is a promising manufacturing process, which could reduce the manufacturing cost, augment the advantages and improve the performance of AGS composite structure. An improved method named soft-mold aided co-curing process which replaces the expansion molds by a whole rubber mold is adopted in this paper. This co-curing process is capable to co-cure a typical AGS composite structure with the manufacturer's recommended cure cycle (MRCC). **N**umerical models are developed to evaluate the variation of temperature and the degree of cure in AGS composite structure during the soft-mold aided co-curing process. The simulation results were validated by experimental results obtained from embedded temperature sensors. Based on the validated modelling framework, the cycle of cure can be optimized by reducing more than half the time of MRCC while obtaining a reliable degree of cure. The shape and size effects of AGS composite structure on the distribution of temperature and degree of cure are also investigated to provide insights for the optimization of soft-mold aided co-curing process.

Keywords: Advanced grid-stiffened (AGS); Soft-mold aided; Co-curing process; Numerical simulation; Thermal analysis.

*Corresponding author:

Dr. Tong Li
School of Chemistry, Physics and Mechanical Engineering
Queensland University of Technology, Brisbane, Australia
Tel.: +61-7-31380225

E-mail address: t14.li@qut.edu.au (Tong Li)

1. Introduction

Advanced grid-stiffened (AGS) composite structures have attracted interests of engineers as replacement materials for honey-comb sandwich and aluminum isogrid structures and they are widely adopted in several business juts, research satellites and the Minotaur launch vehicle [1-3]. AGS composite structures are characterized by a shell (skin) supported by stiffeners (ribs) which run in 2-4 directions along the skin and form a periodically repeating pattern. Generally, the skin and ribs are both made of prepregs where the reinforced fibers are impregnated by thermosetting resin. During curing process of the composite structure, appropriate temperature and pressure provided by a cure cycle are simultaneously applied on the prepregs for an AGS composite structure in an autoclave which initiates the exothermic chemical reaction and squeezes the entrapped void and excess the resin. Owing to the geometrical pattern of ribs and the low thermal conductivity of prepregs, there is a severe internal temperature gradient in the co-curing process which degrades the performance of AGS composite structures. The internal temperature distribution determines the performance of AGS composite structures during the curing process. Low temperature leads to unacceptably long cure time. On the other hand, high temperature can shorten the co-curing time, but may result in residual stress and obvious material degradation. The lower internal temperature gradient leads to unacceptably long cure time. On the other hand, high internal temperature gradient can shorten the co-curing time, but may result in high residual stresses and obvious material degradation.

Some innovative curing processes for the AGS composite structure have been proposed such as hybrid tooling, interlocked composite grids (ICG), and co-curing process. Vasiliev et al. gave a brief introduction on manufacturing and testing as an integral part of development cycle of grid-stiffened structures [4, 5]. Huybrechts et al. introduced a concept of hybrid tooling process using two materials: base tool and expansion block [6]. For a cylindrical AGS composite structure, filament winding is an efficient way for making ribs; a description of manufacture of lattice structures by filament winding along grooves cut in plaster substrates is given by Hou and Gramoll [7]. Kim fabricated an isogrid-stiffened cylinder and an isogrid-stiffened plate with rubber molds during a curing process, and found that the buckling and failure properties of them are excellent while undergoes axial compression [8, 9]. A promising curing process is the co-curing process which fabricates the skin part and the ribs part in a cure cycle [10]. The co-curing process offers the following advantages: (1) larger one-piece structures can be made, joints and discontinuities are reduced, which improves the structural integrity, (2) fewer operations are involved in the manufacturing process, (3) fewer fit-up problems occur, and less sealing is required in assemblies that reduces manufacturing cost.

The soft-mold aided co-curing process which replaces the expansible molds by a rubber mold (as shown in Fig. 1) is one of the most efficient low-cost manufacture techniques for AGS composite structures. To obtain a high quality AGS composite structure, it is critical to draft a proper cure cycle where the aim of co-curing process is to ensure that the resin matrix is evenly distributed and completely cured [11]. A proper cure cycle should not only minimize the accumulated residual stress induced by non-uniform temperature and cure degree, but also control the temperature from approaching thermal degradation and reduce the total process time. The trial and error technique is a general solution for achieving the proper cure cycle for an AGS composite structure, but it is a time and cost-consuming process. Alternatively, based on the mathematical models that describe the variations of prepregs in the co-curing process such as heat transfer, resin flow, fibers compaction, resin cure and stress development, the numerical simulation is an effective and low-cost solution for analyzing the process of co-curing. Although the soft-mold aided co-curing process is a relatively new manufacture technique for AGS composite structures, it could be modelled by referring to the mathematical models for a thick composite plate, as the AGS composite structure is also made of prepregs and heated up with a convection way. Many studies have been carried out to obtain an understanding of the curing phase of resin matrix by numerical modelling methods [12-17]. The heat transfer equations can be solved by the finite difference technique which is convenient for a simple geometry such as flat laminates. However, the solution for the heat transfer equations in a complex geometric part has to resort to the finite element (FE) technique. It is found that the resin manufacturer's recommended cure cycle (MRCC) should be modified to prevent temperature overshoot or reduce the cure time, and a great gradient of temperature can be observed in a flat thick laminates or the heat transfer route in a composite structure [17-19].

Owing to the unique stiffened pattern, soft-mold aided co-curing process for an AGS composite structure is different from the conventional curing process for a composite plate. A uniform thermal conduction route in the composite plate is taken over by a non-uniform thermal conduction route in AGS composite structure and then affects the evolution of mechanical performance. There is limited work on the behaviors of heat transfer and cure kinetics of AGS composite structures which would be affected by molds and the MRCC. Huang, et al, have developed a numerical modelling framework to model the resin flow in normal co-curing process of AGS composite structures [20]. This modelling framework was adopted to study the contribution of composite material property, temperature and AGS structural properties to the physical process of co-curing. The objective of this study is to gain a fundamental understanding of the soft-mold aided co-curing process to improve the manufacture quality of AGS composite structures. In this paper, the variations of temperature profiles inside an AGS composite structure specimen is obtained by numerical simulation during soft-mold aided co-curing process. The simulation results agree well with the monitored results from fiber Bragg grating (FBG) temperature sensors embedded in the AGS composite structure specimen in the co-curing process. Based on the numerical modelling method, an improved cure cycle is proposed to improve the quality of co-curing manufacturing process. Finally, the temperature and cure degree fields in AGS composite structures with different grid shapes and sizes are analyzed by parametric study.

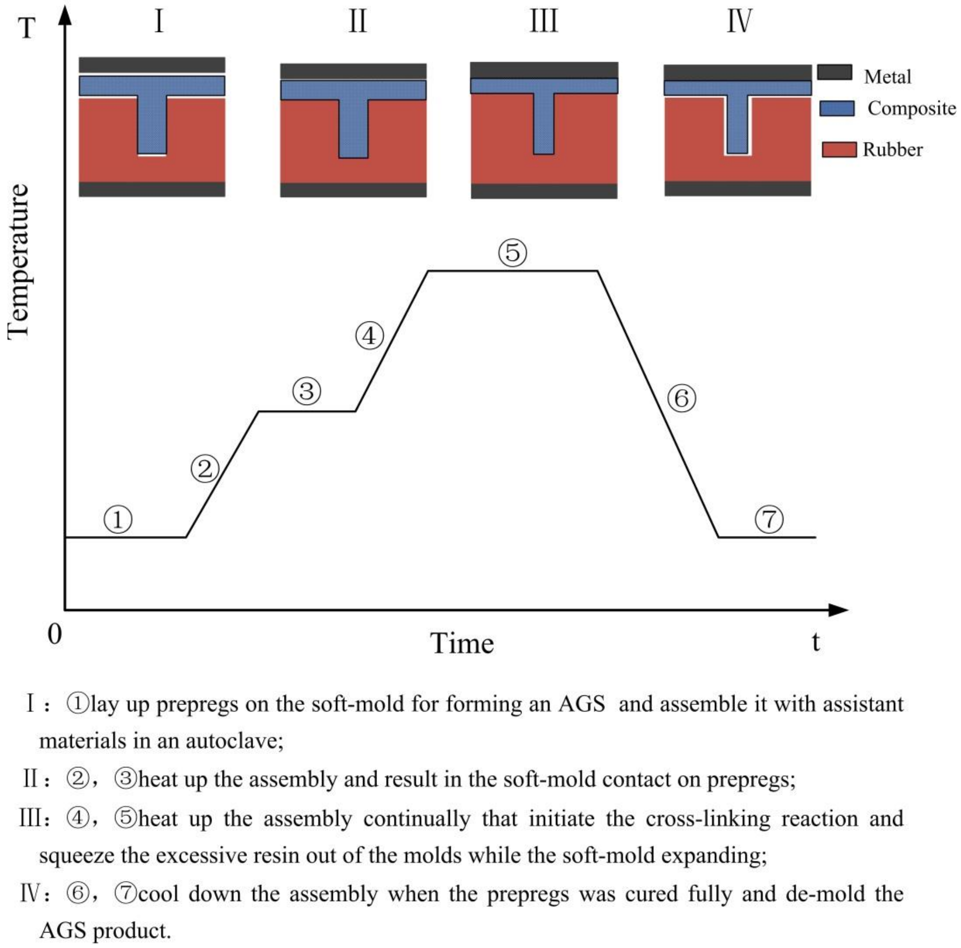

Fig. 1 The principle of soft-mold aided co-curing process for AGS composite structure

2. Thermo-Chemical model

The temperature profiles in an AGS composite structure during the soft-mold aided co-curing process can be obtained through a transient heat transfer analysis including an interior heat source. The combined thermal and cross-linking reaction in resin issue for a given heat cycle is referred to as the primal thermo-chemical analysis. Owing to the slow curing speed, the temperature can be assumed to be in local equilibrium at any time in the prepregs. The differential equation of transient heat transfer with an interior heat source for the prepregs in the co-curing process can be written as follows:

$$\rho c \frac{\partial T}{\partial t} = \frac{\partial}{\partial x_j}\left(k_{ij} \frac{\partial T}{\partial x_j} \right) + \dot{Q} \quad (1)$$

where $\dot{Q}$ is the interior heat source ratio; k_{ij} are the composite anisotropic thermal conductivities; ρ and c are respectively composite density and composite specific heat; and t is the time of thermal conduction.

The interior heat source caused by the cross-linking reaction in resin can be calculated with a cure law of resin. It is expressed as:

$$\dot{Q} = \rho H_r \frac{da}{dt} \quad (2)$$

where α is the cure degree of resin; $d\alpha/dt$ is the rate of cure determined by the cure kinetics of resin; H_r is the heat of reaction of resin in prepregs, defined as the total amount of heat evolved during a complete resin reaction.

Based on the phenomenology, the cure kinetics of a polymer system can be described by the Arrhenius equation and the law of cure degree variation:

$$\frac{d\alpha}{dt} = K(T)\, f(\alpha) \quad (3)$$

where $K(T)$ and $f(\alpha)$ are the Arrhenius equation associated with temperature and the law of cure degree variation, respectively. The law of cure degree variation depends on the resin system, for example, the n-order model is suitable for a resin system while the autocatalytic model is suitable for a polyester system. However, the specific value of the cure kinetics parameters are influenced by the composing of resin means that each type resin has its own cure kinetics.

The cure kinetics for the Glass/Polyester material system can be expressed as:

$$\frac{d\alpha}{dt} = Aexp\left(\frac{-\Delta E}{RT} \right) \alpha^m (1-\alpha)^n \quad (4)$$

where A, ΔE, m and n are the constants of polymer properties whose value determined by fitting the experiment data of differential scanning calorimetry (DSC). A is the pre-exponential factor; ΔE is the activation energy; m and n are the exponential factor of curing; R is the universal gas constant; T is the Kelvin temperature.

The cure kinetics for a Carbon/Epoxy material system can be expressed as:

$$\frac{d\alpha}{dt} = Aexp\left(\frac{-\Delta E}{RT} \right) (1-\alpha)^n \quad (5)$$

where the parameters of A, ΔE, n, R, T and t are the same to the aforementioned parameters.

3. Finite element model

Based on the aforementioned equations, the FE formulations for the thermal problem and cure issue would be derived separately, then combine these formulations to get the complete FE equations for the thermo-chemical model. The FE formulation of Eq. (1) is well documented and the reader is referred to the text by the Reddy [21]. We choose the same FE shape functions $\mathbf{N}(y,z)$ for nodal solution vectors $\mathbf{T}$ (temperature) and α (degree of cure), and approximate the nodal solutions as:

$$T(y,z,t) \approx \mathbf{N}(y,z)\mathbf{T}(t) \qquad \alpha(y,z,t) \approx \mathbf{N}(y,z)\alpha(t)$$

So the FE equations for an element are obtained as:

$$\left[\mathbf{K}_{\mathrm{T}}^{e} + \mathbf{K}_{h}^{e}\right]\left\{\mathbf{T}^{e}\right\} + \left[\mathbf{M}_{\mathrm{T}}^{e}\right]\left\{\frac{\partial \mathbf{T}^{e}}{\partial t}\right\} = \left\{\mathbf{F}^{e}\right\} + \left\{\mathbf{Q}^{e}\right\} \tag{6}$$

$$\mathbf{M}_{\alpha}^{e}\left\{\frac{\mathrm{d}\alpha}{\mathrm{d}t}\right\} = \left\{\mathbf{F}_{\alpha}^{e}\right\} \tag{7}$$

with

$$\mathbf{K}_{\mathrm{T}}^{e} = \iint_{yz}\left(\frac{\partial \mathbf{N}^{\mathrm{T}}}{\partial y} k_{yy} \frac{\partial \mathbf{N}}{\partial y} + \frac{\partial \mathbf{N}^{\mathrm{T}}}{\partial z} k_{zz} \frac{\partial \mathbf{N}}{\partial z}\right)\mathrm{d}y\mathrm{d}z\,, \quad \mathbf{K}_{h}^{e} = \mathbf{N}^{\mathrm{T}} h \mathbf{N}\,, \quad \mathbf{M}_{\mathrm{T}}^{e} = \iint_{yz} \mathbf{N}^{\mathrm{T}} \rho C_{P} \mathbf{N}\mathrm{d}y\mathrm{d}z\,, \quad \mathbf{M}_{\alpha}^{e} = \iint_{yz} \mathbf{N}^{\mathrm{T}}\mathbf{N}\mathrm{d}y\mathrm{d}z\,,$$

$$\mathbf{F}^{e} = \iint_{yz} \mathbf{N}^{\mathrm{T}} \rho H_{u} \frac{\mathrm{d}\alpha}{\mathrm{d}t}\mathrm{d}y\mathrm{d}z\,, \quad \mathbf{F}_{\alpha}^{e} = \iint_{yz} \mathbf{N}^{\mathrm{T}} \frac{\mathrm{d}\alpha}{\mathrm{d}t}\mathrm{d}y\mathrm{d}z\,, \quad \mathbf{Q}^{e} = hT_{\infty}\,.$$

where $\mathbf{K}_{\mathrm{T}}^{e}$ and $\mathbf{K}_{h}^{e}$ are element conductivity and element convection matrices due to conduction and convection, respectively; $\mathbf{M}_{\mathrm{T}}^{e}$ and $\mathbf{M}_{\alpha}^{e}$ are the element capacitance matrices, respectively; $\mathbf{F}^{e}$, $\mathbf{F}_{\alpha}^{e}$ and $\mathbf{Q}^{e}$ are heat load vectors arising from internal heat generation, cure reaction and surface convection. Since both $\mathbf{F}^{e}$ and $\mathbf{F}_{\alpha}^{e}$ depend on $\mathbf{T}$ and α, Eqs. (6) and (7) comprise a transient coupled problem.

Assembly of the elemental contribution and combined with Eq. (7) results in the global system equations:

$$[\mathbf{K}]\mathbf{U} + [\mathbf{M}]\dot{\mathbf{U}} = \mathbf{F} \tag{8}$$

with

$$\mathbf{M} = \begin{bmatrix} \mathbf{M}_{\mathrm{T}} & -\rho \mathbf{H}_{u}\mathbf{M}_{\alpha} \\ 0 & \mathbf{M}_{\alpha} \end{bmatrix}, \quad K = \begin{bmatrix} \mathbf{K}_{\mathrm{T}} + \mathbf{K}_{h} & 0 \\ 0 & 0 \end{bmatrix}, \quad \mathbf{U} = \begin{Bmatrix} \mathbf{T} \\ \alpha \end{Bmatrix}, \quad \mathbf{F} = \begin{Bmatrix} \mathbf{Q} \\ \mathbf{F}_{\alpha} \end{Bmatrix}\,.$$

To solve Eq. (8), the time domain is discretized using the θ method. The solution at the next time step using:

$$U^n = U^{n-1} + [(1-\theta)U^{n-1} + \theta U^n]\Delta t \tag{9}$$

where $\mathbf{U}^n$ and $\mathbf{U}^{n-1}$ are the solutions at the previous and current time steps respectively; Δt is the time step. The parameter θ is an adjustable parameter varying between 0 and 1 and the algorithm depends on the chosen value of θ . If θ between 0.5 and 1, the integration procedures are known as implicit methods. Eq. (10) can be discretized as

$$\left[\frac{\mathbf{M}}{\Delta t} + \theta \mathbf{K}^n\right]\mathbf{U}^n = \left[\frac{\mathbf{M}}{\Delta t} + \left(1-\theta\right)\mathbf{K}^{n-1}\right]\mathbf{U}^{n-1} + \theta \mathbf{F}^n + \left(1-\theta\right)\mathbf{F}^{n-1} \tag{10}$$

Since non-linearity occur from thermal properties and internal heat generation which are dependent on temperature and degree of cure, an iterative procedure is necessary to solve the equations. The Newton–Raphson algorithm, due to its quadratic convergence characteristics, is employed and the tangent stiffness matrix is updated each iteration.

The initial conditions and boundary conditions for the numerical simulation are shown in Eq. (11):

$$\begin{cases} \alpha_i = 0, T_i = T_e \quad at \quad t = 0 \\ T_{boundary} = T_{applied} : mold \quad surface \\ -\lambda_{ij}\dfrac{\partial T}{\partial v} = 0 \; : symmetry \quad boundary \end{cases} \tag{11}$$

where α_i and T_i are the initial cure degree and temperature, respectively; T_e is the environment temperature, i.e. the room temperature; $T_{boundary}$ and $T_{applied}$ are the boundary temperature and the applied temperature on the FE model, respectively.

To verify the solution for simulation the heat conduction of composite in the curing process, A 2-D FE model for a cross section of 2.54 cm thickness unidirection composite plate was developed. The variations of temperature and cure degree during a curing process were simulated by the model with the material system Glass/Polyester, and the simulation results are shown in Fig. 2. According to the Bogetti's work, the boundary conditions are that the top and bottom boundary are the convection boundary condition with a heat transfer coefficient h_T 108.15 $W\cdot m^{-2}\cdot K^{-1}$ while the left and right boundary are adiabtic due to the symmetry, and the thermal and cure kinetic parameters of the Glass/Polymester are shown in Table 1 and Table 2, respectivly [12]. It can be found that the simulation results agree well with the numerical results obtained in literature, and a overshoot is also observed during the second dwell period of cure cycle when a severve cross-linking reaction happened. It could be concluded that the solution could well manifest the variations of temperature and cure degree during the curing process of composites.

Table 1 Thermal parameters of composite and mold

	ρ /(kg/m^3)	C /KJ/(mol·K)	K /W·(m·K)$^{-1}$	
			K_{33}	K_{11}/K_{33}
Silicon rubber	1.23e3	1.53	1.23	1
45# Steel	7.85e3	0.46	50.24	1
Glass/Polyester	1.89e3	1.26	2.163e-4	2
Graphite/Epoxy	1.52e3	9.42e-1	4.457e-4	10

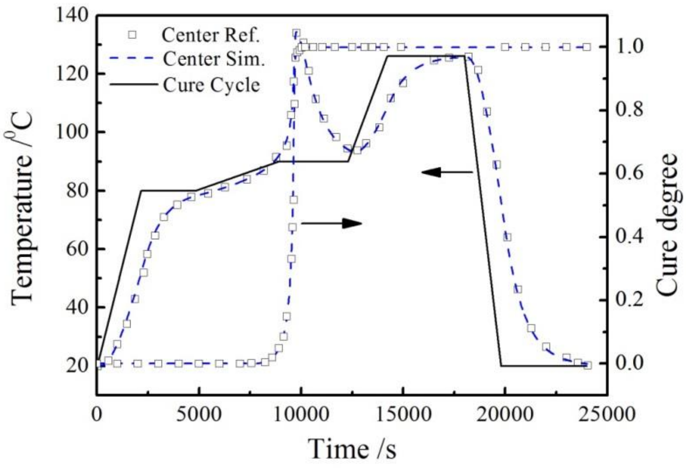

Fig. 2 The simulation results of Glass/Polyester Vs. Bogetti's [12]

Table 2 Cure kinetic parameters for composite

Glass/Polyester [12]		Graphite/Epoxy	
A /min	3.7e22	A /min	7.3e4
ΔE J/mol	1.674e5	ΔE J/mol	59.4e3
m	0.524	H_r J/g	550
n	1.476	n	0.8
H_r J/g	77.5		

4. Experimental validation

It is a time consuming work to locate metal molds for AGS structures during the co-curing process because of complex geometric pattern of ribs. To overcome this drawback, an improved co-curing process named the soft-mold aided co-curing process, in which the molds are replaced by rubber mold, is proposed. The main advantage is to save the process time during the procedure of molds assembly and de-mold. Besides this, the rubber mold is much easier fabricated and designed than other molds due to the flexibility mechanical properties. During the soft-mold aided co-curing process, both the ribs part and the skin part laid-up or wound from prepregs are assembled on a designed rubber mold. Once assembled, the parts are covered with assistant materials such as bleeder and breather, and then sealed inside a vacuum bag. The whole assembly is placed in an autoclave or oven and undergoes a prescribed temperature and pressure cycle.

The mechanical properties of AGS composite structures would be improved by raising the fiber volume fraction due to the pressure from autoclave and the rubber mold with a higher coefficient of thermal expansion (CTE) than other molds. The principle of the soft-mold aided co-curing process is shown in Fig. 1. It can be seen that the prepregs for skin and rib would be cured integrally in one cure cycle and the size of AGS composite structures would be reduced slightly.

The AGS composite structure specimen is stiffened by iso-orthogonal ribs. The soft-mold is made of silicon rubber R-10301 with a higher CTE (provided by the Chengdu Silicon Research Center in China), and the base-plate and the lid-plate are made of steel 45#. The sketch of the soft-mold is shown in Fig. 3, where the rubber is represented by the gray blocks, and the gaps between silicon rubbers represent the grooves for ribs. The materials system of prepregs for the AGS composite structure specimens is the carbon fiber T700 and the epoxy resin 603 provided by the Tory Inc. in Japan and the Aerospace Research Institute of Materials & Processing Technology in China, respectively. The prepregs with the stack sequences $[0/90]_{10s}$ for skin and $[0]_{100}$ for ribs, are laid on the soft-mold by the handing lay-up technique, and then assembled with assistant materials such as Teflon and bleeder. The assembly is bagged with a vacuum bag (shown in Fig. 4), and cured in an autoclave with the resin 603 MRCC. That is, the temperature of air in autoclave is heated up to and dwelled at 135℃ for 1 hour and 190℃ for 4 hours with the rate 25℃/hour respectively, and then cooled down to the room temperature with the ratio -20℃/hour. During the co-curing process, the variation of temperature in the prepregs are monitored by two embedded FBG temperature sensors whit a diameter 0.8mm, which is embedded in the center of a cell skin and the other is embedded in the center of a lateral rib (shown in Fig. 4). The temperature variation of metal lid is also monitored by an additional FBG temperature sensors placed in the lid-plate surface of the assembly. The acquired data is automatically recorded by the optical interrogator device SM130 (provided by the MicronOptics Inc. USA).

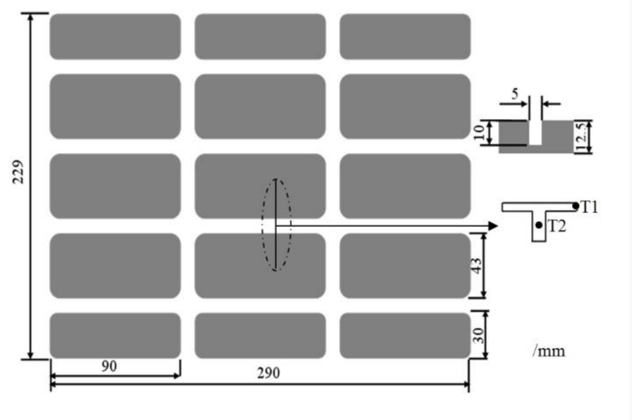

Fig. 3 The sketch of the soft-mold for the soft-mold aided co-curing process

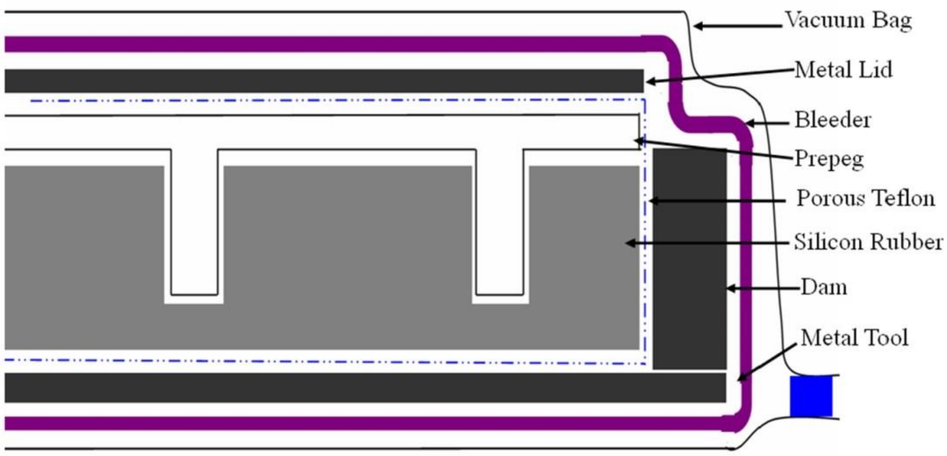

Fig. 4 The sketch of assembly of the soft-mold aided co-curing process for AGS composite structure

Three AGS composite structure specimens are fabricated by the co-curing process and one of the monitored results is shown in Fig. 5. As the cross-linking reaction of resin 603 only happened while the temperature is elevated, the monitored results at the cooling down period are not provided. Due to the low thermal conductivities of soft-mold and a low elevated rate in cure cycle, the temperature of AGS composite structure specimen is increasing gradually without a clear distinction between the temperature elevated periods and the first temperature dwell period. It can be observed that there is not a clearly difference between the monitored results until the AGS composite structure specimen has been cured for about 3 hours, means that there is a uniform distribution of temperature in it and the cross-linking reaction is moderate. As the temperature of AGS composite structure specimen is elevated continually, the cross-linking reaction of resin is intensified and generated a mass of heat which leads to a higher temperature of AGS composite structure specimen comparing to the metal lid temperature. Due to the size of AGS composite structure specimen and the low thermal conductivity of rubber, a temperature overshoot is monitored which happened at the beginning of second temperature dwell period. It can be observed that the temperature difference between skin and rib is over 7℃ at the beginning of second dwell period, and reducing while the co-curing progress. The temperature of skin is close to that of metal lid, because of the higher thermal conductivity of metal. The monitored results illustrate that there is a non-uniform temperature field in the AGS composite structure specimen when it reaches the second temperature dwell period of the MRCC. To ensure that a composite part is fully cured, the MRCC generally takes a lower elevated ratio and longer dwell time which would consume the superiority of co-curing process. The cure cycle for an AGS composite structure should be optimized by some solutions.

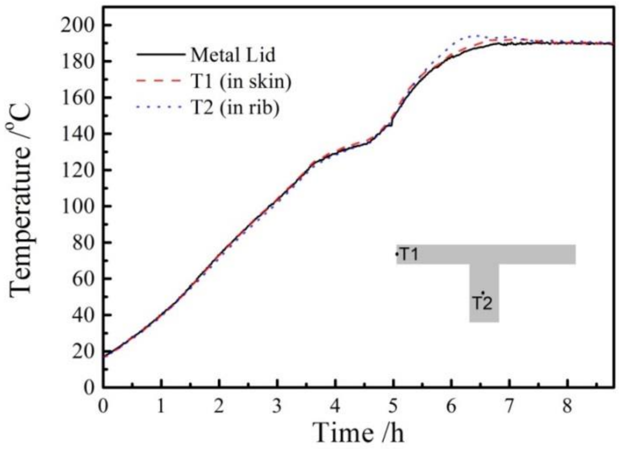

Fig. 5 The monitored results from embedded FBG temperature sensors

5. Results and discussion

According to the collocation pattern of ribs, AGS composite structures can be defined as triangle grid-stiffened composite structure, orthogonal grid-stiffened composite structure, Kagome grid-stiffened composite structure and so on. The AGS composite structure can be denoted by a grid cell shape configuration as shown in Fig. 6(a, b, c), owing to the periodically geometry pattern. The skin part and ribs part are fabricated by prepreg sheets and prepreg tapes, respectively. That is, a sequence of orthogonal prepreg sheets are laid up for the skin part and a sequence of prepreg tapes along the direction of rib are laid up for each rib, respectively. The coordinate indicates that the skin part is laid on the x-y plane while the z axis indicates the thickness of the AGS composite structures. As the fibers in the skin part are orthogonal, there is a section where the properties can be defined as transverse isotropy. Similarly, the fibers in the ribs are unidirectional, there is a section where the properties can also be defined as transverse isotropy. If the sections cross the center of grid (the gray plane in Fig.6), they will be coincide and performing the analysis on the 2-D section is believed to be adequate and appropriate for the AGS composite structures, as the element is symmetric about the cross section and at least one dimension is usually much larger than the other [22]. The temperature gradients in x direction are correspondingly small and can safely be ignored due to the accordance size of ribs in AGS composite structures. As the AGS composite structure's plane dimension is big enough and fibrous bed of prepreg is impregnated with resin, the heat radiation effect in an autoclave can be ignored. Therefore, the whole model can be simplified as a 2-D model. The 2-D model can represent different configurations of AGS composite structures by adjusting the ratio of skin length a/b as shown in Fig. 2(d). The present model is made in the following assumptions:

1. A plane strain condition is assumed to prevail as the size of the AGS composite structure being great

enough;

2. The AGS composite structure is idealized as a void free fiber bed fully saturated with a curing polymer;

3. The thermal properties of the AGS composite structure and molds are constant during the whole co-curing process.

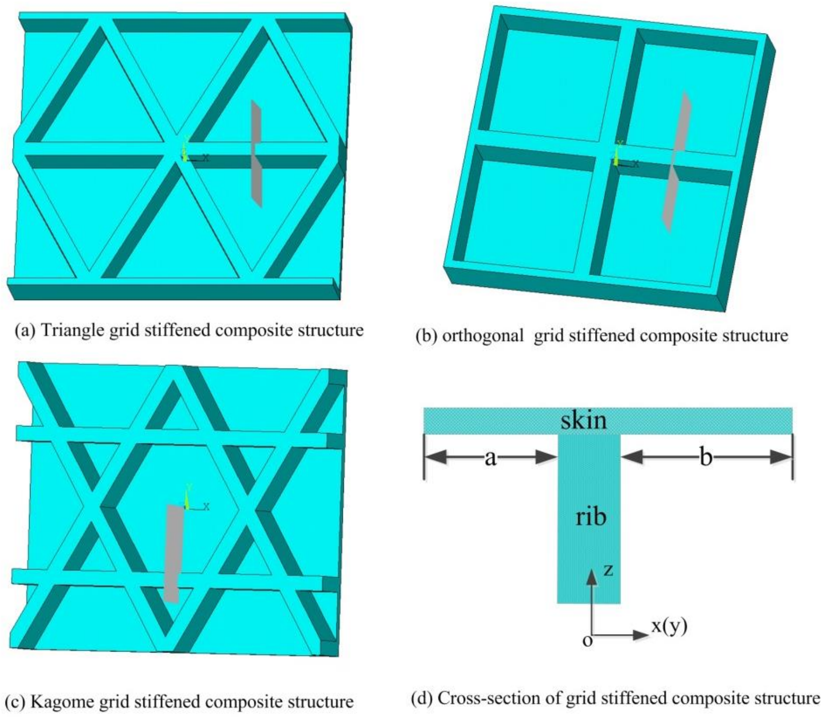

Fig. 6 The typical grid cell shape configuration for AGS composite structures

There are great differences in thermal properties between metal and rubber which is employed as main mold in the soft-mold aided co-curing process for AGS composite structures. Hence, a model for the investigation of co-curing process for AGS composite structures must consider the effect of molds on the composite part that is ignored in previous research. Based on the aforementioned theory and assumptions, the temperature variation of AGS composite structure in the co-curing process could be investigated by a 2-D FE model. Especially, the 2-D FE model would be more efficient than the 3D FE model by reducing the number and node of elements and maintaining an adequate precision. The 2-D FE model including the soft-mold and the metal molds represents the cross-section at the middle of a grid cell. Incorporating with the cure kinetics that is an n-order model provided by the manufacturer of resin 603, the temperature variation of the AGS composite structure specimens in the co-curing process is predicted by a 2-D FE model (shown in Fig. 7). A total 244 nodes and 185 elements are constructed for the AGS composite structure specimen with an 8-node plane strain element. The thermal and cure kinetic parameters required for the simulations are given in Table 1 and Table 2. According to the periodical repeat pattern of the specimen, the boundary conditions are that the left and right border are adiabatic and the top and bottom border are the direct boundary condition means been applied the monitored temperature $T_{metal\text{-}lid}$. Due to the distinction of thermal properties between the composite and rubber, a contact restraint was defined at the interface between these materials, and a constant thermal resistance 50 $W \cdot m^{-1} \cdot K^{-1}$ is considered [23].

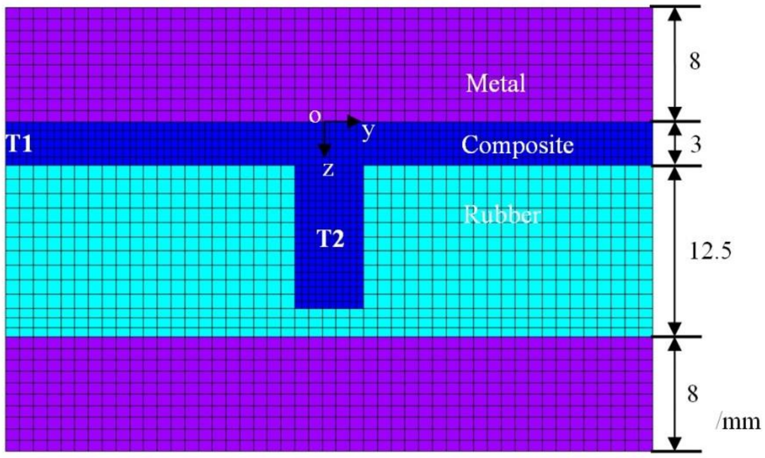

Fig. 7 The 2-D FE model for AGS composite structure specimens

The simulation results for AGS composite structure specimen are shown in Fig. 8 and Fig. 9. It can be seen that the temperature variations in the skin center (T1) and the rib center (T2) agree well with the experimental results. From Fig. 9, there is a uniform distribution of cure degree in the AGS composite structure specimen in the co-curing process, and the final value is over 0.95. The progress of cure degree certifies that the temperature overshoot in the monitored results is caused by the interior heat resource determined by the cross-linking reaction. It can be conclude that, the 2-D FE model can quickly and accurately model the co-curing process for the AGS composite structures.

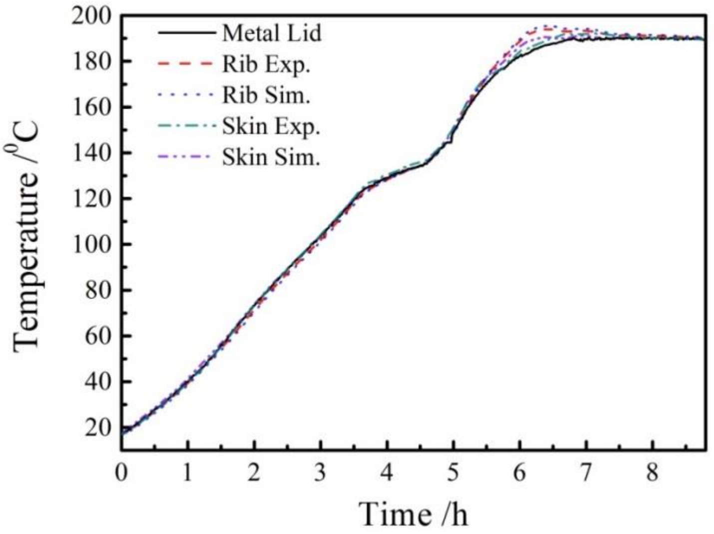

Fig. 8 The simulation temperature profile vs. the experimental results

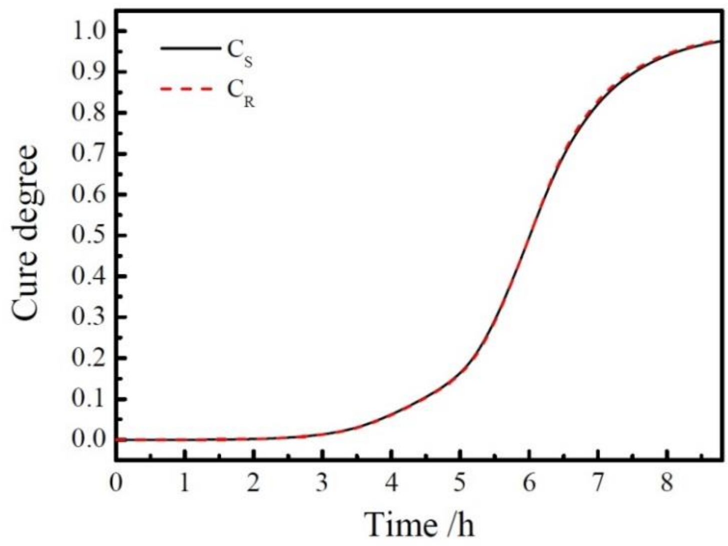

Fig. 9 The variations of cure degree in the AGS composite structure specimen

To save the cost of co-curing process, a reasonable cure cycle is required which could cure an AGS composite structure fully with a less time, i.e. the cure cycle should be adjusted with the parameters according to the size of AGS composite structure, materials system of prepregs, et c. It is ideal to take the method of isothermal curing during a co-curing process for the thermal mismatch. The temperature differences can impact the performance of AGS composite structures, especially in the area between skin and rib. Hence, there must be a moderate distribution of temperature in an AGS composite structure during the co-curing process, because a severe distribution of temperature would accelerate the cross-linking reaction and result to a non-uniform distribution of cure degree which would reduce the performance of AGS composite structure. A reasonable cure cycle is that, there are a less than 5℃ temperature gradient and an over 0.94 cure degree in an AGS composite structure while the co-curing process. Since the numerical simulation employing the proper models that can repeat the calculation of co-curing process with different parameters, it is an efficient method for determining a reasonable cure cycle. Owing to the small size of AGS composite structure specimen and the aforesaid simulation result, the heat rate of cure cycle could be raised to save the processing time and adjust the second temperature dwell period when the mostly cure reaction of resin occurs to ensure the cure degree of AGS composite structure specimen is over 0.94. According to these, an optimal cure cycle is proposed that the AGS composite structure specimen is respectively dwell at 130℃ for 1 hour and 190℃ for 2.5 hours with the heat rate 70℃/hour, and the simulation result is shown in Fig. 10. The optimal cure cycle is 8.5 hours, and the highest temperature is 201℃ which is 11℃ higher than the aim value. The temperature gradient is less than 3℃ during the whole co-curing process. Compared to origin process, the new cure cycle can save the cost of time and improve the quality of products.

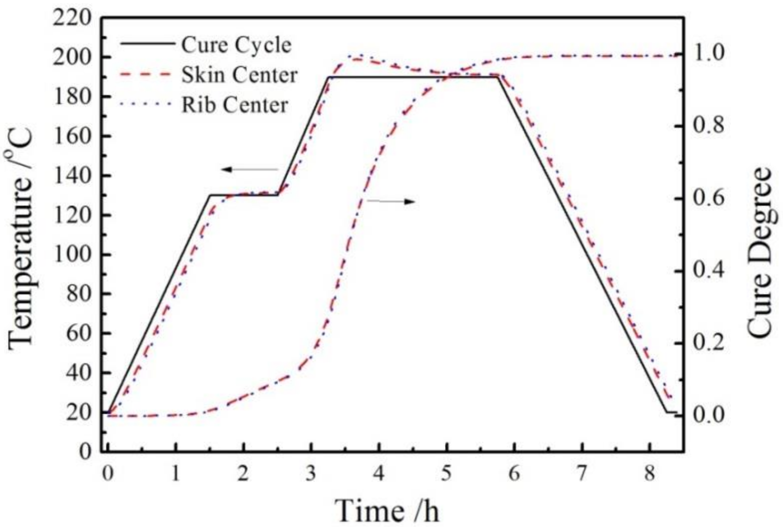

Fig. 10 The temperature and cure degree profiles in the AGS composite structure specimen cured with the modified MRCC

It can be found from Fig. 9 and Fig. 10 that the cure time for the AGS composite structure specimen is reduced to 5.5 hours from the original period of over 8.5 hours, and there are uniform temperature field and cure degree field, which also achieves 0.95 in the co-curing process, and an apparent temperature overshoot is illustrated at the second dwell period of cure cycle.

It can be found from Fig. 11 that the optimal cure cycle save more than 50% time than the origin one which is around 20.3 hours. The quality of the AGS composite structure specimen manufactured by the optimal cure cycle can also satisfy the requirement. The numerical simulation is an effective method to determine an optimal cure cycle for reducing the cost of AGS composite structures.

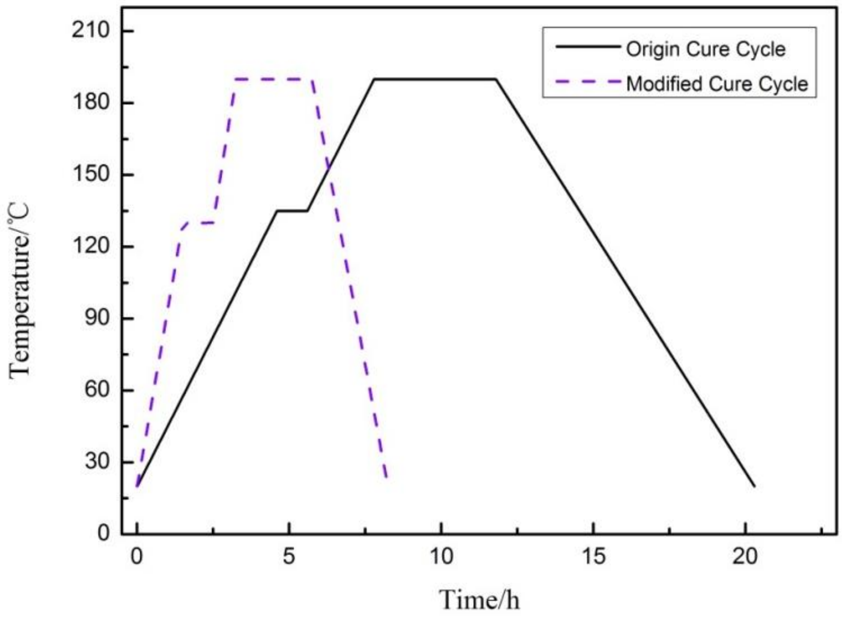

Fig. 11 Different cure cycles in co-curing process

Similarly, the temperature field of an AGS composite structure with another grid pattern also can be investigated by the 2-D FE model. Assume that the ratio of skin length a/b is 2 which indicates that the cross-section within a Kagome grid cell shape (as shown in Fig. 1) and size of skin and ribs is same to further one. The temperature variation of the Kagome grid-stiffened composite structure manufactured by the soft-mold aided co-curing process with the optimal MRCC is shown in Fig. 12. It can be seen that there is a uniform distribution temperature and cure degree field in it and an apparent temperature overshoot arise at the second temperature dwell period of the cure cycle. The contrast among 3 locations in the AGS composite structure model is shown in Table 3. It is obvious that the greatest temperature overshoot happened in location 3 where it is hard for heat dissipation due to its thickness. Three locations cost similar time to reach the overshoot stage. The temperature gradient is under 3℃ in the whole structure. For the different thermal properties between rib and skin, there are large differences between location 1 and 3 or location 2 and 3. The final cure degree of the Kagome grid-stiffened composite structure is over 0.98 which achieves the part quality requirement. However the temperature at skin location is sensitive to the distance from the rib while the temperature overshoot arising. The closer to ribs the more obvious overshoot is observed. It is caused by the great mass of heat generated by the rib and the lower thermal conductivity of the soft-mold and composite. It shows that the 2-D model is also suitable for predicting the temperature distribution in a Kagome grid-stiffened composite cured by the soft-mold aided co-curing process.

Table3 Contrast among 3 locations in the AGS composite structure model

	Location1	Location2	Location3
Overshoot temperature/℃	7.5	8.6	10.5
Time/h	3.679	3.668	3.674
Temperature difference/℃	1.114 (T_2- T_1)	2.495 (T_3- T_2)	2.719 (T_1- T_3)

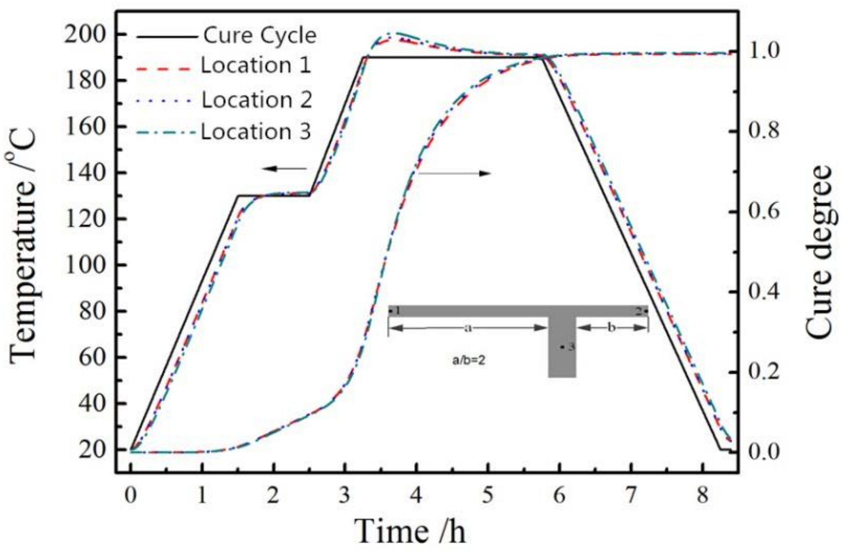

Fig. 12 The temperature and cure degree profiles in a Kagome grid-stiffened composite structure manufactured by the co-curing process

Generally, the curing behavior of composite is sensitive to the size of an AGS composite structure in thickness direction, the bigger size, the more intense gradients of temperature and cure degree fields in it. To investigate the effect of size of an AGS composite structure in the thickness direction on the curing behavior, three different 2-D FE models are developed which enlarges the thickness of skin to 6mm (Model A), and increase the thickness of skin to 6mm and the size of rib to 10×10mm (Model B) and the thickness of skin to 6mm and the size of rib to 5×20mm (Model C). Different cross-sections of the AGS composite structure models are shown in Table 4. According to the 2-D FE model, the profiles of temperature and cure degree of these models are investigated and the results at rib center are shown in Fig. 13. It can be seen that there are distinct temperature overshoot behavior of temperature variation at the second dwell stage of the cure cycle. The more distance from skin surface，the more obvious temperature overshoot is observed. The greatest magnitude of temperature overshoot happened in Model B (17℃ more than Origin Model), rather than Model A and Model C (8℃ more than Origin Model). This shows that the temperature overshoot is not simply dependent on the composite structure thickness, but is related with many factors, such as rib width, soft-mold thermal properties etc. An obviously delay of temperature variation about 0.2h in Model C is observed at the heating and cooling stage. It means that the thickness of AGS structures could delay the outside heat conduction. Although there are distinct profiles of temperature variation at the rib center in these models, the final cure degrees are all over 0.98.

Table 4 The cross-section of the AGS composite structure models

	Origin Model	Model A	Model B	Model C	Model
h_c (mm)	2.5	6	6	6	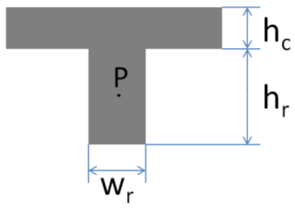
h_r (mm)	10	10	10	20	
w_r (mm)	5	5	10	5	

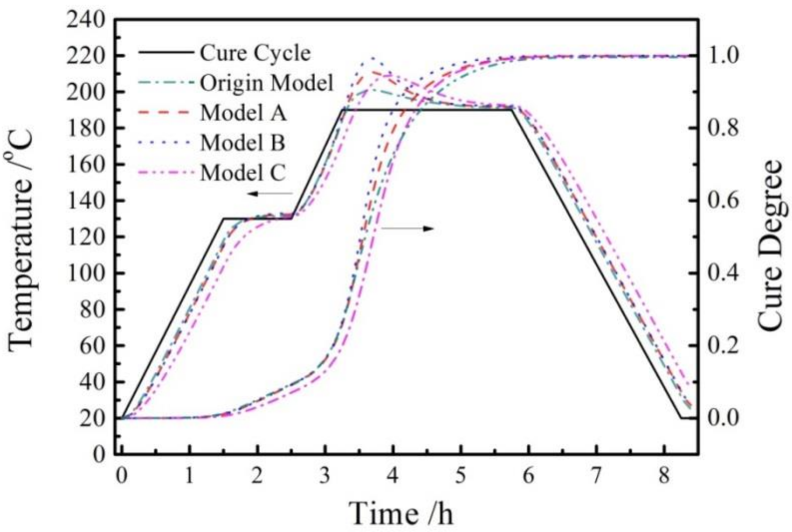

Fig. 13 The temperature and cure degree profiles at rib center of AGS composite structure

Fig. 14 shows the deviations of temperature between rib center and skin center. It can be seen that there is a more even temperature field in Model A than the Original Model. The variation of temperature field in Model B seems that in Model A, except that a more evident temperature gradient is observed at the second dwell stage of cure cycle when the temperature overshoot happened. A greater deviation of temperature (more than 6℃) in Model C is observed, i.e. there is an intense gradient of temperature in Model C. It can be concluded that the curing behavior of an AGS composite structure is more sensitive to the size of rib than the size of skin, and the temperature gradient in AGS composite structure is more sensitive to the height of rib than its width. To ensure the quality of an AGS composite structure manufactured by the soft-mold aided co-curing process, the cure cycle should be adjusted according to the size of rib and skin, especially the height of rib.

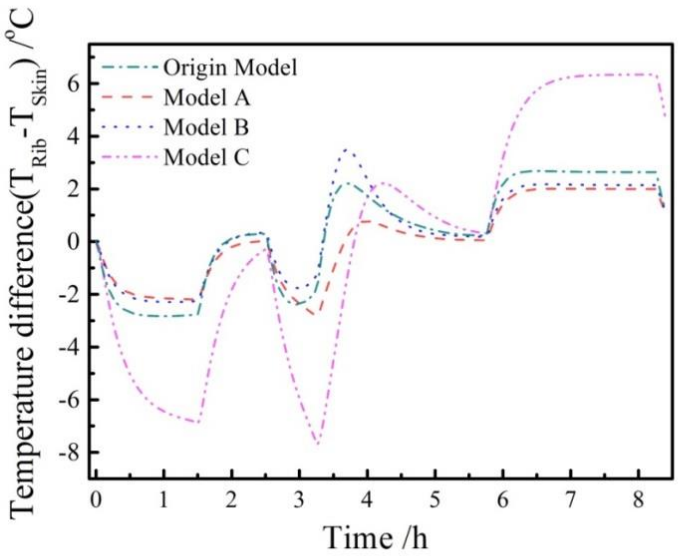

Fig. 14 The temperature difference between the rib and skin in AGS composite structure

6. Conclusions

In the present study, the temperature and degree of cure distributions in AGS composite structures are evaluated using the 2-D FE modelling method during the process of soft-mold aided co-curing. It is found that the modelled temperature profiles agree well with the experimental results obtained by FBG temperature sensors embedded in AGS composite structure specimens. Based on the 2-D FE modelling analysis, the cure cycle is reduced to half the time of MRCC, and the numerical simulation results showed that the AGS composite structure can also be cured fully without intense gradient temperature or cure degree. Although, the 2-D FE model is developed from an AGS composite structure with an iso-orthogonal rib pattern, similar models can also be used for the investigation of AGS composite structures with others resin systems or grid patterns such as triangle, Kagome, and possible future 3D model.

From the modelling results, the distribution of temperature and cure degree fields can be significantly affected by the size of AGS composite structure. The thickness of rib is a major factor for the overshoot of temperature and the height of rib significantly affects the temperature gradient in the material. This modelling framework provides an important tool for the determination of proper cure cycles which improve the quality of soft-mold aided co-curing process for AGS composite structures.

Conflict of Interest Statement

The authors, Mingfa Ren, Qizhong Huang, Changzhi Liu and Tong Li, have no financial and personal relationships that could inappropriately influence or bias this work.

Acknowledgment

This work is supported by the National Basic Research Program of China (No. 2014CB046506，No. 2014CB049000), the National Natural Science Foundation of China (No. 11372058), and the Fundamental Research Funds for the Central Universities (No. DUT13LK28).

References

1. Buragohain, M. and R. Velmurugan, *Study of filament wound grid-stiffened composite cylindrical structures.* Composite Structures, 2011. **93**(2): p. 1031-1038.
2. Sitnikova, E., et al., *Modelling of perforation failure in fibre metal laminates subjected to high impulsive blast loading.* International Journal of Solids and Structures, 2014. **51**(18): p. 3135-3146.
3. Shi, S., et al., *Buckling response of advanced grid stiffened carbon–fiber composite cylindrical shells with reinforced cutouts.* Composites Part B: Engineering, 2013. **44**(1): p. 26-33.
4. Vasiliev, V., V. Barynin, and A. Rasin, *Anisogrid lattice structures–survey of development and application.* Composite structures, 2001. **54**(2): p. 361-370.
5. Vasiliev, V. and A. Razin, *Anisogrid composite lattice structures for spacecraft and aircraft applications.* Composite Structures, 2006. **76**(1): p. 182-189.
6. Huybrechts, S.M., et al., *Manufacturing theory for advanced grid stiffened structures.* Composites Part A: Applied Science and Manufacturing, 2002. **33**(2): p. 155-161.
7. Hou, A. and K. Gramoll, *Fabrication and compressive strength of the composite attachment fitting for launch vehicle.* Journal of advanced materials, 2000. **32**(1): p. 39-45.
8. Kim, T.D., *Fabrication and testing of composite isogrid stiffened cylinder.* Composite structures, 1999. **45**(1): p. 1-6.
9. Kim, T.D., *Fabrication and testing of thin composite isogrid stiffened panel.* Composite Structures, 2000. **49**(1): p. 21-25.
10. Cheung, A., Y. Yu, and K. Pochiraju, *Three-dimensional finite element simulation of curing of polymer composites.* Finite Elements in Analysis and Design, 2004. **40**(8): p. 895-912.
11. Blest, D., et al., *Curing simulation of thermoset composites.* Composites Part A: applied science and manufacturing, 1999. **30**(11): p. 1289-1309.
12. Bogetti, T.A. and J.W. Gillespie, *Two-dimensional cure simulation of thick thermosetting composites.* Journal of Composite Materials, 1991. **25**(3): p. 239-273.
13. Guo, Z.-S., S. Du, and B. Zhang, *Temperature field of thick thermoset composite laminates during cure process.* Composites science and technology, 2005. **65**(3): p. 517-523.
14. Gu, Y., et al., *Numerical simulation and experimental study on consolidation of toughened epoxy resin composite laminates.* Journal of composite materials, 2006. **40**(24): p. 2257-2277.
15. Park, H.C. and S.W. Lee, *Cure simulation of thick composite structures using the finite element method.* Journal of composite materials, 2001. **35**(3): p. 188-201.
16. Capehart, T., H.G. Kia, and T. Abujoudeh, *Cure simulation of thermoset composite panels.* Journal of composite materials, 2007. **41**(11): p. 1339-1360.
17. Oh, J.H., *Cure cycle for thick glass/epoxy composite laminates.* Journal of composite materials, 2002. **36**(1): p. 19-45.
18. Joshi, S., X. Liu, and Y. Lam, *A numerical approach to the modeling of polymer curing in fibre-reinforced composites.* Composites Science and Technology, 1999. **59**(7): p. 1003-1013.
19. Guo, Z.-S., S. Du, and B. Zhang, *Temperature field of thick thermoset composite laminates during cure process.* Composites Science and Technology, 2005. **65**(3–4): p. 517-523.

20. Huang, Q., M. Ren, and H. Chen, *Resin Flow of an Advanced Grid-Stiffened Composite Structure in the Co-Curing Process*. Applied Composite Materials, 2013. **20**(3): p. 303-314.
21. Reddy, J.N., *An introduction to the finite element method*. Vol. 2. 1993: McGraw-Hill New York.
22. Hubert, P., R. Vaziri, and A. Poursartip, *A two-dimensional flow model for the process simulation of complex shape composite laminates*. International Journal for Numerical Methods in Engineering, 1999. **44**(1): p. 1-26.
23. Si, J., et al., *Enhanced thermal resistance of phenolic resin composites at low loading of graphene oxide.* Composites Part A: Applied Science and Manufacturing, 2013. **54**: p. 166-172.